

Radiative Recombination in *p*-Type GaP Doped with Zinc and Oxygen

J. A. W. VAN DER DOES DE BYE

Philips Research Laboratories, N. V. Philips' Gloeilampenfabrieken, Eindhoven, The Netherlands

(Received 3 December 1965)

Visible and infrared luminescence was excited in solution-grown *p*-type GaP(Zn,O) by a pulsed beam of fast electrons (600 kV, 1 mA, 100 nsec). Spectra, intensities, and relaxation times of the emission bands were measured as functions of temperature. The intensities depend linearly on the excitation density. A linear recombination theory can account for the green (2.20-eV), red (1.83-eV), and infrared (1.35-eV) emission bands. The proportionality observed between emission intensity and relaxation time follows from pair recombination of a trapped hole and a trapped electron. A yellow-orange band (2.10-eV) probably connected with the green emission is also discussed. Thermal quenching of the green emission provides the two donor levels involved in the red and infrared emission with electrons. This explains the peculiar decay shapes of the latter bands. It could not be verified whether the red emission involves isolated donor-acceptor pairs, though the radiative transitions do occur between donors and acceptors. The ionization energy spread of the deep donors involved (oxygen, max 0.27 eV) points to clustering of these centers. For the red and infrared emission bands, the weak low-temperature slopes of the intensity and relaxation time versus temperature are caused, respectively, by the weak temperature dependence of the radiationless recombination rate and of the pair recombination rate. The strong high-temperature slopes, which could be measured on the red emission only, are caused by thermal emission from the deep donors concerned. The break point between the weak and strong slopes depends mainly on the radiative recombination rate and the donor trapping rate constant. This explains the invariance of the break point for the samples investigated.

I. INTRODUCTION

THIS paper gives an account of an investigation on radiative recombination processes in *p*-type GaP doped intentionally with zinc and oxygen. This material produces several emission bands under electron bombardment. A pulsed electron bombardment is very useful in the study of the transient properties of the emission. Because the electron beam pulse can be made to have very short rise and fall times very short relaxation times can be measured.

The observations include the well-known red emission band at ≈ 1.8 eV, the green peak at 2.2 eV and its phonon replicas, the slower infrared and yellow-orange luminescence at 1.35 eV and 2.10 eV and the luminescence due to excitons. The intensity and relaxation time of these emissions were observed as functions of temperature.

The typical features that become apparent from measurements under pulsed electron bombardment are:

- (1) An exponential dependence on temperature of the relaxation times and intensities of the emission bands in certain temperature regions; at a definite temperature this exponential temperature dependence changes into a much weaker temperature dependence.
- (2) A near proportionality between the relaxation time and the intensity of the red, infrared, and green emission bands.
- (3) A post-excitation rise prior to decay of the red and infrared emission.

To explain these phenomena a recombination theory is developed for an extrinsic wide-gap semiconductor. It will deal both with stationary and transient recombination.

II. SAMPLE PREPARATION AND EXPERIMENTAL TECHNIQUES

A. Preparation of the Crystals

The samples investigated were obtained by slow cooling of a solution of GaP in Ga with additions of ZnO and Ga₂O₃. The samples labeled Z₄, Z₅, Z₆ in Table I were prepared in a glassy carbon crucible in a sealed ampoule of fused silica Table I(p3) by cooling from 1050°C, and sample 101-139B was prepared directly in a sealed ampoule of fused silica by cooling from 1220°C.

Spectrochemical analysis of the starting material indicated Si and Mg contents of 2×10^{17} – 1×10^{18} at/cm³. This introduces shallow donors and acceptors into the samples in addition to the deliberately introduced centers. Table I contains the data on the Zn¹ and O additions. The concentrations of the effective oxygen centers are not known. The concentration of the well-known donor material sulphur is below 2×10^{16} cm⁻³.

TABLE I. Data on the sample preparation.

Sample	Additions to the Ga melt (at%)		Zinc concentration* (cm ⁻³)	Highest sol. temp. (°C)
	Zn	O		
Z ₄	0.107	0.105	1.5×10^{18}	1050
Z ₅	0.104	0.28	1.5×10^{18}	1050
Z ₆	0.214	0.21	2×10^{18}	1050
101-139B	0.028	0.17		1220

* Evaluated from the additions to the Ga melt according to Ref. 1.

¹ M. Gershenzon, F. A. Trumbore, R. M. Mikulyak, and M. Kowalchik, J. Appl. Phys. **36**, 1528 (1965).

B. Experimental Techniques

The luminescence was excited by a pulsed electron beam of 600 kV with a current of 1 mA onto 1 mm² of sample area. The pulse duration was 100 nsec and the repetition rate 50 cycles/sec. The relaxation times of the emission bands were measured as functions of the temperature. Pulsed excitation was also used to obtain quasistationary emission spectra (See Sec. IVB1). The intensities of these spectra were measured as functions of temperature and excitation density.

The lower limit of measurable relaxation times determined by the transit time spread of the photomultipliers used² was a few nanoseconds. The oscilloscope used was a Tektronix type 585 with plug-in unit type 82 which provides the appropriate bandwidth of ≈ 80 Mc/sec. Frequently it was necessary to prevent overload of the photomultiplier by operation at a reduced high voltage. Additional amplification of the photomultiplier signal was obtained by means of distributed amplifiers³ or by means of a transistorized wide-band amplifier.⁴ The latter amplifier is more suitable for measuring long relaxation times but has considerably more noise. The relaxation times are measured by taking successive half-amplitude points on the oscilloscope screen. The half-times thus obtained from the decay generally increase somewhat with time, so that the decay is not truly exponential.

Measurements were performed down to liquid-nitrogen temperature. The temperature regulation was obtained by controlled liquid-nitrogen injection.⁵

The sample holder accepts four samples which can be brought in turn into the focus of the optical system. This system views the light emission from the side of the sample opposite to the side where the fast electrons impinge. This is done to avoid unwanted luminescence by scattered electrons.

A Leiss monochromator having a focal ratio $f:6.5$ was used with a flint glass prism or with a grating of 15 000 lines per inch. The resolving power of the grating was about 5 meV.

Cathodoluminescence spectra were obtained by two methods which were used simultaneously:

- (1) by direct recording of the photomultiplier output,
- (2) by gate-controlled integration of the luminescence decay curves (time-resolved spectra).

The second of the two methods is used to distinguish between slow and fast components of the spectrum. It eliminates the part of the decay curve that coincides with the excitation pulse and which contains the contributions from Bremsstrahlung and transition radiation. The thermal emission noise from the infrared-sensitive photomultiplier can be suppressed also. In

² RCA trialkali type 7326 for the visible spectrum and Philips type 56 CVP for the near infrared.

³ Instruments for Industry, Inc., Model 530.

⁴ Keithley, Model 104.

⁵ J. A. W. van der Does de Bye, Rev. Sci. Instr. 36, 104 (1965).

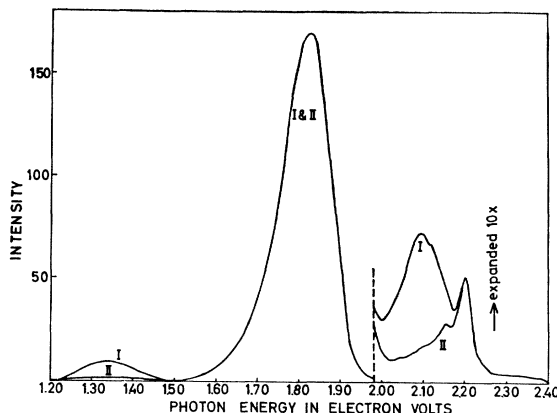


FIG. 1. Emission spectrum of GaP(ZnO) at 80°K. Curve I was taken by direct recording. Curve II was obtained by the method of time-resolved spectra (gated-output integration). It does not contain the slower yellow/orange (2.10 eV) and infrared (1.35 eV) emission bands.

this method the gate pulse cuts out a part of the decay curve which is then transferred to an integration circuit driving a recorder. The gate circuit consists of a long-tailed pair⁶ with the high-slope tubes E 186 F (2X) as the gate tubes and E 810 F (1X) as the signal tube. The required gate pulse is obtained from the gate output of the oscilloscope.

The necessary trigger pulse is excited by the x rays originating from the electron beam pulse, a plastic scintillation phosphor and a normal blue-sensitive photomultiplier being used.

III. MEASUREMENTS

The intensities were found to depend linearly on the current density of the excitation pulse.

Curve I in Fig. 1 shows a typical spectrum taken at

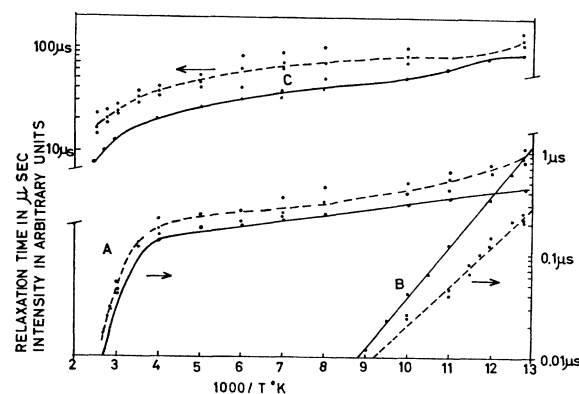


FIG. 2. Temperature dependence of the intensity (—) and relaxation time (---) of the red (curves A), green (curves B), and infrared (curves C) emission bands. Only the τ curves are drawn to the same scale. For every temperature three half-times plotted in the figure were successively measured on the decay curve.

⁶ G. G. Kelley, *Methods of Experimental Physics* (Academic Press Inc., New York, 1964), Vol. 2, p. 344.

TABLE II. Activation energies and peak-height ratios of the emission bands.

Sample	Activation energies of the emission bands (eV)					Peak-height ratios of the emission bands at 80°K		
	Red (E_r)		Green (E_g)		Yellow/orange (E_y)	green/red	yellow-orange/red	infrared/red
	τ	I	τ	I	I			
Z ₄	0.23	0.23	0.085	0.095	≈0.08	0.2	0.2	<0.1
Z ₅	0.22	0.23	0.09	0.085	≈0.08	0.1	0.08	<0.1
Z ₆	0.19	0.18	0.075	0.09	≈0.06	0.05	0.025	<0.1
101-139B	0.28	0.26	0.075	0.10	≈0.06	0.015	0.015	≈0.1

80°K by direct recording; curve II was obtained by gated recording. Curve II consists of a broad red band at ≈1.8 eV and green peaks at ≈2.2 eV and 2.15 eV. The green peaks are known to be a distant pair band and its first phonon repetition.⁷ Curve I contains in addition a slow infrared peak at 1.35 eV and a very slow yellow/orange band at 2.10 eV. These bands have relaxation times much in excess of the gate pulse duration (5 μsec; zero delay). Between the samples investigated no important differences in spectral location of the emission bands were observed. The green emission band peaks at 2.20 eV in all samples. The same impurities are probably involved in this emission.

The semilog plots in Fig. 2 show the near-proportionality between the intensity I and the relaxation time τ for the red (curves A), the green (curves B), and the infrared (curves C) emission bands. Activation energies of both I and τ for the red (E_r) and green (E_g) emission bands as follow from the slopes of the curves are given in Table II. For the yellow-orange band the activation energy (E_y) of only the intensity is indicated as its decay could not be measured. Activation energies will not be derived from the curves of the infrared emission of Fig. 2 because the sloping part is too short to permit a reliable determination.

After the excitation pulse both red and infrared luminescence show a rise prior to decay. This phenomenon of post-excitation rise was found earlier, in weakly doped *p*-type GaP.⁸ For the red emission the rise that occurs during the excitation pulse was clearly observed to have a "parabolic" shape. Figure 3(b) shows the red decay curve together with the electron beam pulse.

The green emission decays monotonically [Fig. 3(a), upper trace].

In Table II the peak-height ratios are given for the emission bands with respect to the red emission of which the efficiency is almost equal for all samples measured. This efficiency was found to be ≈0.2% at room temperature⁹ and consequently (Fig. 2, curve A) is ≈2% at 80°K.

⁷ D. G. Thomas, M. Gershenson, and F. A. Trumbore, Phys. Rev. 133, A269 (1964).

⁸ J. A. W. van der Does de Bye, in *Symposium on Radiative Recombination in Semiconductors, Paris, July 1964* (Dunod Cie., Paris, 1965).

⁹ Thanks are due to Dr. Brill of this laboratory for the determination of the efficiency which was done by comparison with a standard sample.

IV. THEORY

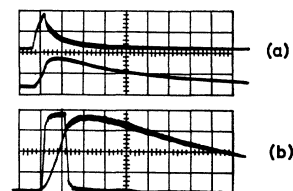
A. Previous Treatments

The curves of intensity and relaxation time in Fig. 2 show strongly and weakly sloping parts. The strongly sloping parts point to thermal emission phenomena while the weakly sloping parts indicate the dominance of weakly temperature-dependent recombination processes.

Most of the green emission bands are due to light emission by distant pairs of shallow donors and shallow acceptors.⁷ A detailed recombination theory for these bands was given by Thomas *et al.*¹⁰ for the case of very low temperatures where thermal emission is absent. The pair distance was found to have a strong influence on the radiative recombination rate. It was possible to explain the green pair bands and, at higher photon energies, the line spectrum by means of Coulomb-energy corrections. The influence of the pair distance on the recombination rate explains the strongly nonexponential decays observed on distant pair bands.

In the temperature region of the present investigation the thermal emission of trapped electrons, however, dominates the radiative recombination yielding the green emission. This implies a different kind of decay which contains a much weaker influence of the pair distance especially on the ionization energies of the donor and the acceptor in the pair. In view of the small width of the green peaks the approximation of these energies by single values may be allowed for the theoretical treatment of recombination. This use of single values implies a single value for the Coulomb-energy correction. This correction can be inferred from emis-

FIG. 3. (a) Decay curves of the green (upper trace) and red (lower trace) emission. Time scale, 0.2 μsec/cm. (b) The "parabolic" rise of the red emission during the excitation pulse, which is also shown, and its post-excitation rise. Time scale, 0.1 μsec/cm.



¹⁰ D. G. Thomas, J. J. Hopfield, and K. Colbow, in *Symposium on Radiative Recombination in Semiconductors, Paris, July 1964* (Dunod Cie., Paris, 1965).

sion spectra¹¹ to be between 25 and 30 meV, which corresponds to a mean pair distance of $\approx 50 \text{ \AA}$.

Maeda¹² developed a nonlinear recombination theory for weakly doped material. In this theory the concentrations of isolated distant pairs were used as variables and single values for the ionization energies were assumed.

The pair concept with the assumption of single values for the ionization energies will also be used in this paper. The present investigation is especially concerned with the luminescence of strongly doped materials at temperatures above liquid-nitrogen temperature. The validity of the pair concept for these materials will also be examined.

The red emission was ascribed by Gershenson *et al.*¹ to pair recombination of carriers trapped on deep donors (oxygen) and shallow acceptors (zinc). Strong phonon cooperation was supposed to broaden the emission band. This phonon cooperation makes the determination of the Coulomb-energy correction impossible.

B. A Linear Pair-Recombination Theory

1. Basic Assumptions

In the present theory the pair concept and the assumption of a single value for the Coulomb-energy correction will be maintained. The theory will be concerned with two observables, i.e., the emission intensity at stationary excitation and the relaxation time at pulsed excitation, both as functions of temperature. The excitation will be assumed to be homogeneous throughout the sample. Actually stationary intensities were not measured directly but derived from emission spectra obtained by pulsed excitation. The linear behavior of the material on excitation allows the interpretation of these intensities as stationary intensities.

Apart from isolated pairs unpaired centers occur which being "true" traps have no influence on the stationary behavior. Unpaired donors, however, being minority carrier traps in a *p*-type material may have a profound influence on the transient behavior. In extrinsic *p*-type material nonequilibrium holes will occur in concentrations that are much lower than the thermal equilibrium values so that holes trapped on unpaired acceptors need not be taken into account.

Comparison of the mean pair distance¹¹ for the green emission ($\approx 50 \text{ \AA}$) with the mean distance between the acceptors in GaP with $\approx 10^{18} \text{ cm}^{-3}$ acceptors ($\approx 100 \text{ \AA}$) allows the conclusion that in such material all "green" donors are paired. The mean pair distance for the red emission is not known. It will be assumed, however, that all donors relevant to the red emission are also paired with acceptors.

The green emission at low temperatures and the red emission at high temperatures can be treated separately

¹¹ F. A. Trumbore and D. G. Thomas, Phys. Rev. **137**, A1030 (1965).

¹² K. Maeda, J. Phys. Chem. Solids **26**, 595 (1965).

because use can be made of the fact that the effect of thermal emission on the green and red luminescence lies in different temperature regions (see Fig. 2). This simplifies the theory in the following way:

First, at the temperatures where the green emission is observable trapping by the deep "red" donors and subsequent radiative transition parallels the recombination of electrons from the conduction band with other levels. These two parallel mechanisms can therefore be taken together as one mechanism. The solutions for the green emission case can then be obtained. They also lead to the description of the red emission for the temperature region considered. This description contains the explanation of the peculiar rise and decay of the red emission (see Fig. 3).

Secondly, at higher temperatures where thermal emission from the "red" donors dominates the behavior of the red emission no appreciable fraction of the excited electrons will be trapped on the shallow "green" donors. Consequently these donors will then play no role any more in the treatment of the red emission.

2. General Solutions

The four possible cases, viz., one or both carriers present or absent in a pair, make it possible to distinguish four different kinds of isolated pairs with concentrations α , β , γ , and δ (see Fig. 4). The δ pairs may yield light by the recombination of the trapped electron and the trapped hole. In strong *p*-type material only pairs containing empty donors occur in thermal equilibrium, i.e., only α and γ pairs are present. The sum of their concentrations approximately equals the total pair concentration (N_0).

Linearity requires the excited concentrations $\Delta\alpha$ and $\Delta\gamma$ to be small compared to the equilibrium values α_0 and γ_0 . In wide-gap material $\Delta\delta$ and $\Delta\beta$ are larger than δ_0 and β_0 . Similar inequalities can be given for the free-carrier concentrations, i.e., $\Delta p \ll p_0$ and $\Delta n \gg n_0$. Therefore, $\Delta\alpha$, $\Delta\gamma$, and Δp need not be taken into account so that only three variables $\Delta\delta$, $\Delta\beta$, and Δn remain to describe the transitions. In the case of transient behavior these variables depend on time.

From the level and transition scheme of Fig. 4 three simultaneous linear differential equations follow:

$$\begin{aligned} U(t) - d\Delta n/dt &= (R_x + D)\Delta n - I_a\Delta\delta - I_a'\Delta\beta, \\ -d\Delta\delta/dt &= -B\gamma_0\Delta n + (R + I_a + I_a')\Delta\delta - A\Delta\beta, \\ -d\Delta\beta/dt &= -B'\alpha_0\Delta n - I_a\Delta\delta + (I_a' + A)\Delta\beta, \end{aligned} \quad (1)$$

in which $U(t)$ is the rate of excitation of electrons from the valence band to the conduction band. Only band-band excitation is assumed to take place. D is the rate of electron trapping by the donors in the α and γ pairs. It is equal to $[B\gamma_0 + B'\alpha_0]$ in which B and B' are the trapping-rate constants. The unspecified transition rate R_x is included to describe transitions of free electrons to levels from which no thermal emission occurs. It

may contain both radiative and radiationless transitions. R is the radiative transition rate of the δ pairs.

The thermal emission terms I_d and I_d' are different because the ionization energy present in I_d' is smaller than that of I_d owing to the repulsion by the Coulomb field of the ionized acceptor which is present in the β pair. This field also causes a difference between the trapping-rate constants B and B' . These rate constants also occur in the expressions for I_d and I_d' ¹³:

$$\begin{aligned} I_d &= BN_c \exp(-E_d/kT), \\ I_d' &= B'N_c \exp(-E_d'/kT). \end{aligned} \quad (2)$$

A and I_a are trapping and thermal emission rates of the acceptors. The terms A' and I_a' differ from A and I_a owing to the Coulomb field of the ionized donor. A' and I_a' control the equilibrium between γ_0 and α_0 and therefore do not appear in Eqs. (1). A and A' are proportional to p_0 .

The Laplace transformation

$$\bar{f}(s) = \int_0^\infty \exp(-st) f(t) dt \quad (3)$$

is used to obtain an algebraic expression for the set of Eqs. (1):

$$\begin{aligned} \bar{U}(s) &= (s+R_x+D)\Delta\bar{n}(s) - I_d\Delta\bar{\delta}(s) - I_d'\Delta\bar{\beta}(s), \\ 0 &= -B\gamma_0\Delta\bar{n}(s) + (s+R+I_a+I_d)\Delta\bar{\delta}(s) - A\Delta\bar{\beta}(s), \\ 0 &= -B'\alpha_0\Delta\bar{n}(s) - I_a\Delta\bar{\delta}(s) + (s+I_d'+A)\Delta\bar{\beta}(s). \end{aligned} \quad (1a)$$

By means of Cramer's rule the relevant solutions are found to be

$$\begin{aligned} \Delta\bar{\delta}(s) &= \frac{\bar{U}(s) \begin{vmatrix} B\alpha_0 & -A \\ B'\alpha_0 & (s+I_d'+A) \end{vmatrix}}{D(s)} \\ &= \bar{U}(s) M_{n\delta}(s)/D(s), \end{aligned} \quad (4a)$$

$$\begin{aligned} \Delta\bar{n}(s) &= \frac{\bar{U}(s) \begin{vmatrix} (s+R+I_a+I_d) & -A \\ -I_a & (s+I_d'+A) \end{vmatrix}}{D(s)} \\ &= \bar{U}(s) M_{nn}(s)/D(s). \end{aligned} \quad (4b)$$

In each solution the minor is the cofactor of the variable in the first row of the determinant of Eqs. (1a):

$$D(s) = \begin{vmatrix} (s+R_x+D) & -I_d & -I_d' \\ -B\gamma_0 & (s+R+I_a+I_d) & -A \\ -B'\alpha_0 & -I_a & (s+I_d'+A) \end{vmatrix}. \quad (5)$$

In the case where $U(t)$ is a delta or a step function, $\bar{U}(s)$ is respectively a constant or proportional to $1/s$.¹⁴ The solutions may then be directly obtained when the roots of $D(s)$ are known.

¹³ The (unknown) multiplicity factor is not introduced into these expressions.

¹⁴ The proportionality constant is the excitation rate U_{st} , which appears at time $t=0$ and then remains constant.

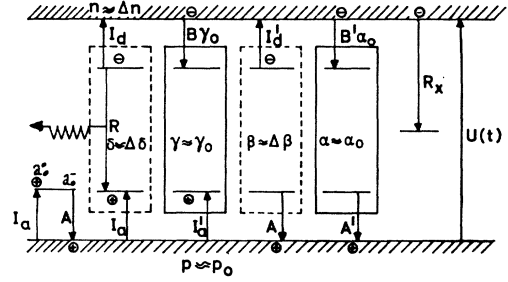


FIG. 4. Level and transition scheme to describe one emission band (green or red) of GaP(Zn,O) containing the four different kinds of pairs of donors and acceptors with the concentrations δ , γ , β , and α . The δ and β pairs dotted in the figure only occur by excitation in p -type material. Their concentrations are given as $\Delta\delta$ and $\Delta\beta$. Likewise the free-electron concentration is given by $\Delta n \approx n$. The excess concentrations of the other pairs are small compared with the equilibrium values γ_0 and α_0 so that $\gamma \approx \gamma_0$ and $\alpha \approx \alpha_0$. Likewise the concentrations of free holes and of holes trapped on unpaired acceptors a remain nearly constant so that $p \approx p_0$ and $a^o \approx a^o_0$. Unpaired donors are assumed to be absent. The thermal emission rates I_d' and I_a' and the trapping-rate constants contained in $B'\alpha_0$ and A' are modified by the Coulomb field of the charged center opposite to the center in the pair considered.

The final solutions are sums of the exponential functions $A_i \exp(-r_i t)$, in which the r_i 's are the relaxation rates or reciprocals of the observable relaxation times (for the case of linear behavior). This implies the occurrence of the terms $1/(s+r_i)$ in the Laplace transforms. Three relaxation rates r_i exist, being the roots of the third-order determinant $D(s)$ which can be expressed by the equalities

$$D(s) = \Pi(s+r_i) = s^3 + a_2 s^2 + a_1 s + a_0, \quad (5a)$$

in which

$$a_2 \approx r_1, \quad a_1 \approx r_1 r_2, \quad \text{and} \quad a_0 \approx r_1 r_2 r_3,$$

by virtue of the assumed inequality

$$r_1 \gg r_2 \gg r_3. \quad (6)$$

The coefficients r_1 , $r_1 r_2$, and $r_1 r_2 r_3$ are obtained from the determinant [Eq. (5)];

$$r_1 = R_x + D + R + I_d + I_d' + I_a + A, \quad (7a)$$

$$\begin{aligned} r_1 r_2 &= [(R_x + D)(I_a + A) + I_d'(R_x + B\gamma_0) \\ &\quad + I_d(R_x + B'\alpha_0) + I_d I_d' + I_d A + I_a I_d'] \\ &\quad + R[(R_x + D) + (I_d' + A)], \end{aligned} \quad (7b)$$

$$\begin{aligned} r_1 r_2 r_3 &= R_x [I_d I_d' + I_d A + I_a I_d'] \\ &\quad + R[A(R_x + D) + I_d'(R_x + B\gamma_0)]. \end{aligned} \quad (7c)$$

By means of the theorem¹⁵

$$\lim_{t \rightarrow \infty} f(t) = \lim_{s \rightarrow 0} s \bar{f}(s) \quad (3a)$$

the solutions for the stationary case may be derived from the transient solutions (4) by putting $s=0$ and using the stationary excitation function U_{st} . $D(s)$ then

¹⁵ G. Doetsch, *Anleitung zum praktischen Gebrauch der Laplace-Transformation* (Oldenbourg, München, 1956), p. 117.

reduces to

$$D(0) = r_1 r_2 r_3. \quad (5b)$$

The solutions for the stationary case now become

$$\Delta\delta = U_{st}[AD + I_d' B\gamma_0]/r_1 r_2 r_3, \quad (4c)$$

$$\Delta n = U_{st}[(R + I_d)(I_d' + A) + I_a I_d'] / r_1 r_2 r_3. \quad (4d)$$

The practice of putting $s=0$ to obtain stationary solutions can be used to simplify the transient solutions also when the smaller relaxation times $1/r_1$ and $1/r_2$ are shorter than the rise and fall times of the excitation pulse. This is equivalent to saying that r_1 and r_2 are larger than s . The determinant (5a) then reduces to

$$D(s) = r_1 r_2 (s + r_3). \quad (5c)$$

$$I/(\tau dU_{st}) = \frac{R[AD + I_d' B\gamma_0]}{(R_x + D)(I_a + A) + I_d'(R_x + B\gamma_0) + I_d(R_x + B'\alpha_0) + R(I_d' + A)}. \quad (8a)$$

To obtain the required constant value, approximations which retain I_d and I_d' are not useful because rather unrealistic assumptions for the multiplying terms in Eq. (8a) would then have to be made.

The approximation that no longer contains I_d and I_d' is

$$I/(\tau dU_{st}) = R \frac{D}{R_x + D} \frac{A}{A + I_a}. \quad (8b)$$

For the derivation of this equation from Eq. (8a) use was made of the assumptions

$$(R_x + D) \gg (I_a + A) \gg (R + I_d) \quad (\text{Ref. 16}) \quad (9a)$$

and

$$A \gg I_d'. \quad (9b)$$

By means of equilibrium statistics it will be shown in Sec. IVB5 that $A/(A + I_a)$ in Eq. (8b) is nearly constant. This implies a constant hole concentration on the acceptors. A discussion on the proportionality will be given in Sec. VIII.

The inequalities (9) also simplify the remaining coefficients r_1 and $r_1 r_2 r_3$ of Eqs. (7). This leads to the three relaxation rates

$$r_1 = R_x + D, \quad (10a)$$

$$r_2 = I_a + A, \quad (10b)$$

$$r_3 = \frac{A}{A + I_a} \left[R + \frac{R_x}{R_x + D} (I_d + I_d' I_a / A) \right]. \quad (10c)$$

The first term within the brackets of Eq. (10c) is related to the weakly sloping part of the τ -versus- T curve for the red emission in Fig. 2. The second term

¹⁶ The pair recombination rate R which actually depends on the pair distance is averaged here over the entire emission band.

3. Intensities and Relaxation Times

To simplify the expressions (7) for r_1 , $r_1 r_2$, and $r_1 r_2 r_3$ use can be made of the near-proportionality observed between the intensity I and the relaxation time τ . The relevant equation follows from Eq. (4c):

$$I/\tau = dR\Delta\delta r_3 = U_{st} dR M_{n\delta}(0) / r_1 r_2 \quad (8)$$

in which the intensity $I = dR\Delta\delta$ (photons/sec cm²); d is the thickness of the sample; τ is the reciprocal of the smallest relaxation rate r_3 .

Proportionality, hence a constant value for I/τ , requires simplification both of $M_{n\delta}(0)$ and $r_1 r_2$. It certainly necessitates the removal of the constant terms and the products of the exponentially temperature-dependent rates I_d , I_d' , A , and I_a from the expression (7b) for $r_1 r_2$. This leads to

contains the exponentially temperature-dependent rates I_d and I_d' and demonstrates in the same curve the effect of thermal emission. The ratios $A/(A + I_a)$ and I_a/A will be found later to be temperature-independent (see Sec. IVB5). Equation (10b) indicates the speed of exchange of holes between the acceptors and the valence band and hence the speed of transition between the δ and β pairs.

From the Eqs. (8b) and (10c) the expression for the intensity follows:

$$I = R d \Delta \delta = \frac{U_{st} d D}{R_x + D} \frac{R}{R + [R_x / (R_x + D)] [I_d + I_d' I_a / A]}. \quad (11)$$

From the Eqs. (10c) and (11) it is seen that τ and I show the same behavior on temperature variation. The break point between the weakly and strongly sloping parts is also the same. An expression from which the break point temperature T_b can be derived follows from the Eqs. (10c) or (11):

$$[I_d + I_d' I_a / A] / R = (R_x + D) / R_x \quad (12)$$

with the use of the expressions (2) for I_d and I_d' . This will be done at the end of Sec. V. It is found that, depending on the degree of compensation,

$$E_d / k T_b \approx \ln(N_c B / R), \quad (13a)$$

$$E_d' / k T_b \approx \ln(N_c B' / R). \quad (13b)$$

4. Transient Behavior

This section will be mainly concerned with the post-excitation rise observed on the red and infrared emission bands.

The equation which describes the post-excitation

rise has to contain an expression of the type $[\exp(-r_i t) - \exp(-r_j t)]$ which starts and ends at zero. The Laplace transform of this equation will then contain $[(s+r_i)(s+r_j)]^{-1}$. Two relaxation rates are thus involved.

It was mentioned earlier (Sec. III) that the post-excitation rise of the red luminescence may be caused by thermal emission of electrons from shallow donors and subsequent retrapping by deeper donors. This means an increase of the electrons on the red donors also after termination of the excitation. The deeper donors are directly involved in the radiative transitions yielding the red emission.

During the excitation pulse the electron concentration on the "green" donors has an approximately linear rise and so has the thermal emission and retrapping flow to the "red" donors.¹⁷ Consequently the electron concentration on the latter donors increases parabolically and so causes the "parabolic" rise observed on the red emission.

It was pointed out in Sec. IVB1 that the green luminescence which involves the shallow donors can be treated separately for the temperatures where the post-excitation rise of the red emission occurs. This means that the solution for the red emission can be obtained from the (separate) treatment of the green luminescence. The latter treatment is required to yield the concentration $\Delta\bar{n}(s)$ of excited free electrons, part of which is now trapped by the "red" donors. The concentration of the electrons trapped by the "red" donors $\Delta\delta(s)$ follows from this $\Delta\bar{n}(s)$ by means of the relation

$$\frac{\Delta\delta(s)}{\Delta\bar{n}(s)} = \frac{M_{ns}(s)}{M_{nn}(s)}. \quad (14)$$

This relation is obtained from the general solutions (4). The inequalities (9) and the determinant (5c) are used to obtain¹⁸

$$\Delta\delta(s) = \frac{D_r}{R_k + D_g + D_r} \frac{A_r}{A_r + I_{ar}} \frac{\bar{U}(s)}{s + r_r} \times \left[1 + \frac{D_g}{R_k + R_g + D_r} \frac{I_g}{s + r_g} \right], \quad (4e)$$

and

$$\Delta\bar{n}(s) = \frac{\bar{U}(s)}{R_k + D_r + D_g} \left[1 + \frac{D_g}{R_k + D_r + D_g} \frac{I_g}{s + r_g} \right], \quad (4f)$$

in which

$$r_g = I_g [R_k + D_r] / [R_k + D_r + D_g], \quad (15)$$

with

$$I_g = [I_{ag} I_{ag}' + A_g I_{ag}] / [I_{ag} + A_g], \quad (16)$$

$$r_r = R_r A_r / [I_{ar} + A_r], \quad (17)$$

¹⁷ The assumed linearity implies that the donors are not saturated by excitation.

¹⁸ The subscripts r and g are introduced to distinguish between symbols relevant to the red and green emission.

and

$$R_k + D_r = R_x; \quad (18)$$

r_g and r_r are both derived from the general expression (10c).

The solution for $\Delta\delta(s)$ contains the product $[(s+r_g)(s+r_r)]^{-1}$ that expresses the post-excitation rise. The bracketed term in the expression (4e) and (4f) for $\Delta\delta(s)$ and $\Delta\bar{n}(s)$ should be larger than unity, i.e., the "green" trapping rate D_g should not be small compared with the sum of the "red" trapping rate D_r and the free-electron recombination rate R_k . The "parabolic" rise of the red emission also follows from the same solution of Eq. (4e) if the transform for an excitation pulse of finite duration is used for $\bar{U}(s)$.

Equation (4f) for $\Delta\bar{n}(s)$ consists of a part containing s which implies decay with relaxation time $1/r_g$ (the slow part) and a part without s which follows the excitation function closely (the fast part). These two parts are of equal importance when a post-excitation rise is observed. Consequences of this will be discussed later in connection with fast-exciton emission (Sec. VII).

5. The State of Thermal Equilibrium

The state of thermal equilibrium of p -type material will be treated in order to obtain expressions for $A/(A+I_a)$ and I_a/A which appear in Eqs. (8b) and (10c). This treatment involves the accented terms I_a' and A' .

A high degree of compensation causes the Coulomb field in the donor-acceptor pair to become relatively important. This entails a weak temperature dependence of the ratios mentioned above.

An expression for I_a/A will be derived below, assuming that only one type of donor is involved and that all donors are paired with acceptors.

The ratio of α_0 (concentration of empty pairs) to γ_0 (concentration of pairs with one trapped hole) follows from the level scheme of Fig. 4:

$$\alpha_0/\gamma_0 = I_a'/A'. \quad (19a)$$

This ratio equals $\exp[(E_F - E_a')/kT]$ omitting multiplicity factors. E_a' is the acceptor binding energy E_a minus a mean Coulomb energy of the pairs (ΔE).

A similar relation can be found for unpaired acceptors with concentration a :

$$a^-/a^0 = I_a/A = \exp[(E_F - E_a)/kT]. \quad (19b)$$

With the assumptions

$$N_a^- = a^- + \alpha_0 \approx N_d; \quad N_a^0 = a^0 + \gamma_0 \approx (N_a - N_d) \gg p_0 \quad (20)$$

and

$$\alpha_0 + \gamma_0 \approx N_0 \approx N_d \quad (\text{all donors are paired}) \quad (21)$$

and putting $I_a/A = z$; $I_a'/A' = cz$ [in which c is the Coulomb term, $\exp(\Delta E/kT)$] the following relation is found.

$$z(1+cz)/(1+z) = N_d/(N_a - N_d) \quad (22)$$

which, at a high degree of compensation reduces to

$$cz \approx N_d / (N_a - N_d). \quad (22a)$$

The value of ΔE to be applied in this relation is much lower than the mean Coulomb-energy correction that is relevant to the luminescence band considered (i.e., 25–30 meV for the “green” pairs; see Sec. IV.A). The large number of the distant pairs which contribute a small fraction to the emission band then has to be fully taken into account. Probably the Coulomb term c approaches unity so that relation (22) reduces to

$$z = N_d / (N_a - N_d) \quad (22b)$$

for all degrees of compensation. This relation also applies to materials in which different types of donors are paired with the same type of acceptors if the assumption $c \approx 1$ holds for the different types of pairs. The different donor-ionization energies then depend in the same way on the compensation degree but possibly with different Coulomb-energy corrections.

The assumption of $(N_a - N_d) \gg p_0$ in Eqs. (20) remains to be checked. When $\ln p_0$ (majority concentration) versus reciprocal temperature can be approximated by straight lines which intersect at break points a relation can be found for the break point at the temperature where saturation sets in:

$$E_a/kT_b \approx \ln(N_a/N_d). \quad (23)$$

This relation is approximately valid for any degree of compensation.¹⁹ At the highest temperature investigated (400°K) a constant value of z requires N_a to be at least $3 \times 10^{18} \text{ cm}^{-3}$ assuming $E_a \approx 0.04 \text{ eV}$ and $N_v \approx 10^{19} \text{ cm}^{-3}$. The value for N_a is close to the total concentration of shallow acceptors (Zn and Mg). (See Sec. II.A.)

V. COMPARISON OF EXPERIMENTAL AND THEORETICAL RESULTS

The expressions for τ and I (10c) and (11) rewritten with $I_a/A = z$ are

$$\tau = (1+z)[R + (I_a + zI_a')R_z / (R_z + D)]^{-1}, \quad (10d)$$

and

$$I = \frac{D}{R_z + D} \frac{U_{st}d}{1 + [(I_a + zI_a')/R][R_z / (R_z + D)]} \quad (11a)$$

[in which $I_a \sim \exp(-E_a/kT)$ and $I_a' \sim \exp(-E_a'/kT)$, see Eqs. (2)]. These equations give rise to strongly sloping and horizontal parts in the curves for τ and I versus T . They give a qualitative account of the red emission curves in Fig. 2. The activation energy of τ and I is seen to change from E_a to $E_a' = E_a - \Delta E$ with increasing compensation. Hence the isolated pair concept allows different values for the activation energy. The theory predicts the same activation-energy value

for both τ and I if the quantities in Eq. (8b) (I/τ ratio) are constant. The “green” intensity seems to have a somewhat higher activation energy than the “green” relaxation time (see Table II). The difference is about 10 meV and may be caused by the weak temperature dependence in the electron recombination rate R_z , to be dealt with later in this section. Such a difference could not be found for the steeply sloping parts of the red emission curves owing to the insufficient accuracy of measurement.

The same weak temperature dependence in R_z causes the change of the (theoretical) horizontal part of the $\ln I$ -versus- $(1/T)$ curve into the weakly sloping part of the curve actually observed (Fig. 2). The relevant expression for this part follows from Eq. (11a):

$$I = U_{st}dD_r / (D_r + R_k). \quad (11b)$$

The weakly sloping parts of $\ln \tau$ and $\ln I$ versus $1/T$ have nearly the same slope. The part of the τ curve is described by

$$\tau = (1+z)/R \quad (10e)$$

which follows from Eq. (10d). As z was found to be constant (Sec. IVB5) a temperature dependence of R must be involved. Thus there is a difference between the red and the green emission. For the latter it was found that the pair recombination rate does not depend on temperature.^{10,12}

The mechanism proposed for the post-excitation rise of the red emission (Sec. IVB4) involves thermal emission from the “green” donors. It requires the equality of the “red” rise time and the “green” decay time, both being the reciprocal of the “green” relaxation rate τ_g . It has not yet been possible to confirm this equality experimentally.

The quantum efficiency η defined as $\eta = I / (U_{st}d)$ can be derived from Eq. (11a). For the red emission in the low-temperature region this leads to

$$\eta_r = D_r / (D_r + R_k). \quad (11c)$$

It can be shown that η_r changes into

$$\eta_r' = D_r / (D_r + D_g + R_k) \quad (11d)$$

at the very low temperatures where the green emission efficiency (η_g) attains its maximum value.

The combination of the change from η_r to η_r' and the weak temperature dependence of R_k should lead to a maximum in the red emission efficiency. For the samples of the present investigation this maximum probably occurs at a temperature below liquid-nitrogen temperature. A maximum was actually observed by Gershenzon.¹

The relations for the break-point temperature (T_b) mentioned in Sec. IVB3 can be expressed in such a way as to contain the quantum efficiency. Equation (12) leads to the following expressions:

$$E_d/kT_b = \ln(N_e B/R) + \ln(1 - \eta_r), \quad (13c)$$

¹⁹ The multiplicity factor is unknown and taken to be 1.

and

$$E_d'/kT_b = \ln(N_c B'/R) + \ln(1 - \eta_r) + \ln[N_d/(N_a - N_d)], \quad (13d)$$

for low and high compensation, respectively.

For the red emission case the left-hand term of Eq. (13c) and Eq. (13d) amounts to about 10. It is immediately seen that the red emission efficiency (η_r) must be very close to unity to cause the break point to occur at higher temperatures. The last term of Eq. (13d) shows that a high degree of compensation shifts the break point to lower temperatures. As η_r is rather low the invariance of the break point for the samples investigated points either to a low or to an invariant degree of compensation. It is seen that the break point mainly depends on the quantity $N_c B/R$ (or $N_c B'/R$) which is not influenced by the amount of radiationless transitions.

For the determination of the trapping rate constant B (or B') of the donors the high-temperature part of Eq. (10d) can be rewritten as follows:

$$1/\tau = (1 - \eta) B N_c \exp(-E_d/kT). \quad (10f)$$

The values derived from the τ curves of Fig. 2 are for the "red" donors $\approx 10^{-8}$ cm³/sec and for the "green" donors $\approx 10^{-7}$ cm³/sec. Hence the "green" donors trap more strongly than the deeper, "red" donors. No good quantitative theory for trapping rates is known to the author.

VI. COMPARISON OF THE DIFFERENT SAMPLES

Some of the observations on the samples investigated are summarized in Table III.

It will be investigated whether the spreads of the values of E_r , E_g , and τ_r can be explained by differences in the degree of compensation on the basis of the isolated pair theory. No correlation between the "red" relaxation time τ_r and the activation energies E_r and E_g (Ref. 20) can be established using Eqs. (10a) and (11a) which involve the degree of compensation. This degree of compensation is unknown by lack of data on the donor concentrations. The small spread of the τ_r values means that either the degree of compensation is nearly the same for all samples or the red emission does not involve isolated pairs which contain shallow acceptors. In both cases the large spread of the E_r values has to be explained by a different mechanism. A different electrostatic influence which also depresses an activation energy is produced by the reduction of the donor ionization energy by neighboring donors.²¹ This reduction depends on the distance between donors and is counteracted by the screening from charged acceptors which are close to the donors. This does not fully account for the large spread of E_r values because the

²⁰ The spread of the E_g values is below the known Coulomb-energy correction of 0.025–0.030 eV (Sec. IVA) and is not large compared with the accuracy of measurement.

²¹ P. P. Debye and E. M. Conwell, Phys. Rev. **93**, 193 (1954).

TABLE III. Emission strengths, activation energies, and relaxation times.

Sample	Emission strength		Activation energy		τ_r (sec) at 80°K
	green	red	E_r (eV)	E_g (eV)	
Z ₄	strong	very strong	0.23	0.09	1×10 ⁻⁶
Z ₅	strong	very strong	0.23	0.09	1×10 ⁻⁶
Z ₆	moderate	very strong	0.19	0.075–0.09	7×10 ⁻⁷
101-139B	weak	very strong	0.27	0.075–0.10	1.1×10 ⁻⁶

E_g values still have a small spread. A nonrandom distribution may have to be assumed for the "red" donors to obtain short distances between these donors. As both types of electrostatic influence reduce the activation energy of donors the highest values 0.09 and 0.27 eV found for E_g and E_r may be close to the true donor binding energies. The former value also follows from the $(E_a + E_g)$ sum that can be found to be ≈ 0.14 eV from the spectral location of the green peak (at 2.20 eV). Owing to the large width of the red emission band it is not possible to establish a similar correlation for the red emission.

The E_r value of 0.27 eV of 101-139B nearly equals the value of 0.28 eV found by Gershenzon¹ for the binding energy of a doubly ionized oxygen donor in compensated *n*-type material. The value of 0.23 eV, however, is more frequently measured. Because the red emission always occurs when shallow acceptors and oxygen are present, it is reasonable to assume that radiative transitions involve these shallow acceptors and that oxygen causes the deep donor level.

VII. ADDITIONAL EMISSION PHENOMENA

Only the red and green emission were compared with the theory (Sec. V). It has therefore to be investigated whether the theory proposed is affected by the other simultaneously occurring luminescence phenomena, i.e., the fast exciton and the slow yellow-orange and infrared luminescence.

The infrared emission also has a post-excitation rise and a near-proportionality between I and τ ; the post-excitation rise probably has the same cause as that of the red emission. Both effects indicate that the infrared emission also derives from transitions from donors to acceptors.

The different relaxation times of the two emission bands imply two different minority carrier populations and hence two different donor levels. The "infrared" donor level is probably deeper than the "red" donor level as the infrared emission does not decrease much with increasing temperature. The acceptor levels involved may be the same or different. As the thermal emission from the "infrared" donors seems to be negligible the recombination process giving the infrared emission may be thought to be included in the radiationless recombination rate (R_x) and therefore does not affect the theory of the red and green emission.

For the yellow/orange emission all samples showed nearly the same, temperature-independent ratio between the "green" and "yellow/orange" intensities (see Table II) which indicates a close coupling between the two emission processes. Because of the different speeds of the two processes, however, two different donor levels must be involved. A direct transfer of electrons from the "green" to the "yellow/orange" donor or a reabsorption of a "green" photon exciting an electron from the valence band into the latter donor may have to be considered.

The fast luminescence with $h\nu \approx E_{gap}$ has exactly the same time behavior as the excitation pulse. This luminescence can not derive from free electrons as according to Sec. IVB4 free electrons do not follow the excitation pulse closely. The luminescence has been ascribed to a donor-bound exciton emission and its phonon replicas.^{22,23} The donor was assumed to be split off from a higher conduction band. This assumption is thus supported by the time behavior found.

VIII. GENERAL DISCUSSION

The stationary and transient luminescence phenomena can be satisfactorily described in terms of radiative transitions of electrons from donors to acceptors.

The temperature dependence of both observables, luminescence intensity and relaxation time, indicates the presence of thermal emission from minority carrier trapping levels, i.e., donors in *p*-type material; this explains sufficiently the strongly sloping parts of the *I*- and τ -versus- $1/T$ curves (Fig. 2). In the weakly sloping parts the radiative recombination predominates.

The "red" donors are much deeper than the "green" donors so that thermal quenching of the red emission must occur at higher temperatures.

The rather close proportionality between both observables found for the green and red luminescence indicates that:

(1) Thermal emission and (radiative) recombination transitions should start from the same minority carrier trapping level so that donors are directly involved in the radiative recombination process in *p*-type GaP. Thermal emission from these donors would increase the speed with which trapped electrons disappear from the donors, decreasing the radiative electron flow proportionally.

(2) Radiative transitions should end in a level which has a constant hole concentration. This involves either shallow acceptors in a high concentration or an acceptor level which lies several times kT above the Fermi level in the entire temperature region. The required shallow acceptor concentration could have been provided by Zn and Mg together.

²² D. G. Thomas, M. Gershenson, and J. J. Hopfield, *Phys. Rev.* **131**, 2397 (1963).

²³ M. Gershenson, in *The Physics of the III-V Compounds* (to be published).

There are two other frequently used recombination mechanisms that, however, do not lead to proportionality:

(A) A mechanism in which radiative transitions involve free electrons released by donor traps, a mechanism frequently assumed in recombination models for II-VI compounds. This mechanism implies a decrease of the relaxation time and an increase of the luminescence at increasing thermal emission.

(B) A mechanism in which the ground state of a donor traps an electron which is then thermally emitted to an excited state of this donor. The latter state is involved in the radiative transition of the electron. This mechanism resembles mechanism (A). They even become indistinguishable when the free electrons and the electrons on the excited states have the same quasi-Fermi level.

The recombination theory (Sec. IV) was developed for isolated pairs but this approach does not restrict the applicability to an isolated pair model only. The trapped electrons were divided into two different groups, i.e., two different kinds of isolated pairs. The indistinguishability between these trapped electrons presents the case that a trapped electron may recombine with an arbitrary hole trapped on an acceptor level. The theory for the latter case is thus a simplification of the theory presented.

The two conclusions from the proportionality do not require the radiative transitions to occur within isolated pairs. These conclusions could be drawn for a model in which a trapped electron is able to recombine with an arbitrary hole present on an energy level which has a constant hole concentration. Recombination of a trapped electron with a free hole is precluded as the free hole concentration is not constant in the temperature region of the present investigation. In such a case an observed I/τ proportionality can be regarded as a proof for recombination of bound electrons with bound holes.

A constant hole concentration implies that the lower temperature slope of the "red" emission intensity cannot be explained by thermal depopulation of the acceptors.¹ That this is not possible is also apparent from the efficiency equations (11c) and (11d) which do not contain an acceptor property. Actually these equations state that in the relevant temperature regions excited electrons are distributed over radiative and radiationless transitions in a ratio which contains the donor trapping rates and the radiationless recombination rate only. The lower temperature slopes of the *I* curves (Fig. 2) result from a temperature dependence of the radiationless recombination rate.

Using two exponential functions of time containing the "green" and "red" relaxation times, the theory accounts for the "parabolic" rise of the red emission intensity during the excitation pulse and the post-

excitation rise. These features of the luminescence decay curve are consequences of the retrapping by the "red" donors of electrons thermally emitted into the conduction band from the "green" donors. This mechanism also explains the maximum of the red emission intensity versus temperature mentioned in Sec. V. The explanation of these phenomena does not require the radiative recombination to occur within isolated pairs. As a consequence of the theory developed the "red" rise time and the "green" decay time should be equal. The method of measurement limits the accuracy with which these times could be determined. With this restriction an inequality of the times mentioned above could not be established for the GaP(Zn,O) samples investigated.

The case of recombination of a trapped electron with an arbitrary hole bound to an acceptor, mentioned earlier in this section, implies that the radiative recombination rate is proportional to the concentration of neutral acceptors. This concentration probably varies

from sample to sample. Therefore neither this kind of recombination nor the isolated pair theory seem to be able to account for the large agreement between the various samples in time behavior of the red emission at low temperatures. This time behavior remains to be explained. An explanation should also account for the slight temperature dependence of the red emission decay and be compatible with the assumption of donor aggregation proposed to explain the large spread in the deep donor ionization energy (see Sec. VI).

ACKNOWLEDGMENTS

The author wishes to acknowledge the helpful discussions with Dr. Klasens, Dr. Diemer, Dr. Knippenberg, H. J. Vegter, and Dr. Grimmeiss. He is indebted to Dr. Knippenberg for a critical reading of the manuscript. The samples were provided by H. J. Vegter, P. Verhoog, and P. H. J. M. Verberne assisted in carrying out the experiments.

Scattering of Conduction Electrons by Localized Surface Charges

R. F. GREENE AND R. W. O'DONNELL

U. S. Naval Ordnance Laboratory, Silver Spring, Maryland

(Received 29 December 1965)

The differential scattering probability w_s for conduction electrons scattered by localized surface charges is calculated using the Born approximation. This is applied to a recently derived expression for the Fuchs reflectivity parameter p in terms of w_s . In a typical (semiconductor) case, the reflectivity p is an order of magnitude closer to unity than is the kinetic specularity W_0 (=probability of a specular reflection). A strong angular dependence of p is shown to be a compromise between an "aspect effect" and a "termination effect," with the latter usually dominant. The "termination effect" is the partial suppression of the scattering matrix element produced by terminating the wave function at the crystal surface. The "aspect effect" is the increase in the number of surface scatterers seen by a de Broglie wave front of unit diameter when it is turned toward glancing incidence. The dominance of the "termination effect" produces unit reflectance p at glancing angles.

I. INTRODUCTION

QUANTITATIVE treatments of surface and size effects in metals and semiconductors are usually based on the Boltzmann-Fuchs method,^{1,2} in which the space-dependent Boltzmann equation is solved with the Fuchs boundary condition (b.c.). This b.c. is

$$f_1(v_z) = p f_1(-v_z) \text{ at } z=0+, \text{ with } 0 \leq p \leq 1, \quad (1)$$

where f_1 is the nonequilibrium part of the electronic distribution function $f = f_e + f_1$. Customarily, the reflectivity p is an empirical constant, chosen to give the best fit of theory to experiment, and representing in some sense the extent to which electrons are specularly reflected rather than randomly scattered at the surface.

Various mechanisms have been proposed² for the origin of surface scattering and, in this paper, we calculate p for one of these mechanisms: scattering by localized surface charges. This scattering differs from the corresponding bulk process because the wave function is terminated by the crystal surface. This partially suppresses, as pointed out by Ham and Mattis,³ the overlap matrix element of the scattering potential for electrons having a small normal velocity component. This "termination effect" may be expected to produce a strong angular dependence in p , as noted by Aubrey, James, and Parrott.^{4,5}

¹ F. S. Ham and D. C. Mattis, IBM J. Res. Develop. 4, 143 (1960).

² J. E. Aubrey, C. James, and J. E. Parrott, *Proceedings of the International Conference on Semiconductor Physics, Paris, 1964* (Dunod Cie, Paris, 1964), p. 689.

³ J. E. Parrott, Proc. Phys. Soc. 85, 1143 (1965).

¹ E. H. Sondheimer, Advan. Phys. 1, 1 (1952).

² R. F. Greene, Surface Sci. 2, 101 (1964).